Uncoupled human flavin-containing monooxygenase 3 can release superoxide radical in addition to hydrogen peroxide

Gianluca Catucci, Chongliang Gao, Giulia Rampolla, Gianfranco Gilardi and Sheila J. Sadeghi*

Department of Life Sciences and Systems Biology, University of Torino, Italy

* Corresponding author: Department of Life Sciences and Systems Biology, Via Accademia Albertina 13, 10123 Torino, Italy.
Tel.: +39 011 6704528
Fax: +39 011 6704643
E-mail address: sheila.sadeghi@unito.it

Abstract

Human flavin-containing monooxygenase 3 (hFMO3) is a drug-metabolizing enzyme capable of performing N- or S-oxidation using the C4a-hydroperoxy intermediate. In this work, we employ both wild type hFMO3 as well as an active site polymorphic variant (N61S) to unravel the uncoupling reactions in the catalytic cycle of this enzyme. We demonstrate that in addition to H_2O_2 this enzyme also produces superoxide anion radicals as its uncoupling products. The level of uncoupling was found to vary between 50 and 70% (WT) and 90 to 98% (N61S) for incubations with NADPH and benzydamine over a period of 5 or 20 minutes, respectively. For the first time, we were able to follow the production of the superoxide radical in hFMO3, which was found to account for 13-18% of the total uncoupling of this human enzyme. Moreover, measurements in the presence or absence of the substrate show that the substrate lowers the level of uncoupling only related to the H_2O_2 and not the superoxide radical. This is consistent with the entry point of the substrate in this enzyme's catalytic cycle.

These findings highlight the importance of the involvement of hFMO3 in the production of radicals in the endoplasmic reticulum, as well as the relevance of single-nucleotide polymorphism leading to deleterious effects of oxidative stress.

Keywords: flavin-containing monooxygenase, hydrogen peroxide, superoxide radical, polymorphic variant, N61S, uncoupling.

1. Introduction

Human flavin-containing monooxygenase 3 (hFMO3) is a drug metabolizing enzyme expressed at high levels in the human liver [1-3]. Human FMO3 is the major human enzyme able to perform the monooxygenation of trimethylamine (TMA) yielding trimethylamine N-oxide (TMAO) [4]. Impaired metabolism of its main substrate TMA is known to cause trimethylaminuria, a genetic disease in which affected individuals present high levels of TMA in both sweat and urine leading to a displeasing body odor [5,6]. The disease is caused by mutations of the hFMO3 gene that cause an altered activity of the enzyme and have direct consequences on the oxidation of TMA. One such mutation, N61S, leads to a polymorphic variant known to cause trimethylaminuria [7]. On the other hand, the product of the reaction, TMAO, was recently found to be a risk factor for cardiovascular disease [8-10].

Previous characterization of pig liver FMO has shown how FMO is reduced by NADPH and upon binding of O_2 it can form a stable long-lived C4a-hydroperoxyflavin intermediate [11,12]. This species reacts very well with soft nucleophiles performing a monooxygenase reaction, followed by the formation of water and the release of the oxidized $NADP^+$ cofactor [11,12]. Nevertheless, recent work carried out with purified human FMO1, FMO2, FMO3 and FMO5 have demonstrated how the human enzyme does not seem to form a long-lived intermediate and that the detachment of oxygen species from peroxyflavin might lead to uncoupling [13- 16]. The uncoupling reaction, which is defined as the wastage of electrons and oxygen without oxidation of the substrate, can lead to the formation of reactive oxygen species (ROS) such as the superoxide radical and/or hydrogen peroxide. Earlier studies performed with pig FMO have highlighted the formation of superoxide anion radical at the rate of about 4% the total NADPH oxidized [17]. Formation of hydrogen peroxide, up to 41% of the total NADPH oxidized, has also been demonstrated in earlier work with purified rabbit lung FMO [18]. However, more

79 recently the human FMOs 1, 2 and 3 were found to release only H_2O_2 after reduction by NADPH
80 with no superoxide radical being observed [16].
81 In this work, since we had previously purified hFMO3 [19] and its polymorphic N61S variant
82 [13], we set out to measure the uncoupling products of these enzymes in order to clarify whether
83 the human enzyme also produces the superoxide radical or only hydrogen peroxide. To do so,
84 we tested the ability of the enzyme to use the electrons provided by NADPH to perform the
85 monooxygenation reaction, by quantifying both the amount of ROS (hydrogen peroxide and
86 superoxide radical) and product formed. The N61S polymorphic variant was selected due to its
87 poor binding affinity for $NADP^+$ leading to an acceleration of the C4a-hydroperoxyFAD
88 intermediate decay [13], resulting in higher uncoupling.
89
90 **2. Material and Methods**
91 2.1 Cloning, expression and purification
92 The pJL2-hFMO3 plasmid constructed previously [19, 20] was used with QuikChange® site-
93 directed mutagenesis kit (Stratagene) to produce N61S hFMO3 [13]. Human FMO3 gene
94 containing a C-terminal poly-histidine tag was heterologously expressed in *E. coli* cells and
95 purified as described previously [21]. The protein was stored at -80 ºC in 50 mM KPi pH 7.4,
96 20% glycerol with 1 mM EDTA. Protein purity and concentration was determined
97 spectroscopically as described previously [13, 22].
98 2.2 NADPH oxidation, hydrogen peroxide and superoxide detection
99 All the reactions were carried out in the dark, in triplicates, in 96-well plates using a plate reader
100 equipped with a uv-vis absorbance detector using 1.6 μM hFMO3, 160 μM NADPH and 0 or
101 300 μM benzydamine in 50 mM KPi pH 7.4. The optical pathlength was 0.45 cm. The plate
102 reader automatically takes into account the optical pathlength on the basis of the volume used

in the 96-well plates. For NADPH consumption reactions, mixtures were incubated at 37 °C. NADPH signal at 340 nm was monitored in time using 6220 M^{-1} cm^{-1} as extinction coefficient. Preliminary controls were performed to establish reaction conditions that do not lead to undesired production of hydrogen peroxide by NADPH autoxidation. The controls are shown in Figure S1 where incubations of AMPLEX RED kit are reported with or without NADPH. Results indicate that under our experimental conditions there is no detectable contribution to hydrogen peroxide formation by NADPH. Basal NADPH consumption in the absence of the substrate was also tested (Figure S2).

Potential interference of benzydamine with the Amplex Red assay was evaluated by comparing identical assay conditions in the presence or absence of benzydamine. Figure S3 shows that there is no interference with the assay.

For every assay aimed at the quantification of hydrogen peroxide the amount of hydrogen peroxide in the unknown sample was determined using a calibration curve prepared with fresh hydrogen peroxide and run in parallel with the unknown samples.

For H_2O_2 detection 50 µL of reaction mixture was withdrawn from a well at each time point and mixed in an eppendorf containing 50 µL of cold acetonitrile to terminate the reaction, centrifuged at 14000 rpm for 5 minutes and subjected to HPLC separation. The remaining 50 µL of reaction mixtures were incubated with AMPLEX RED [16, 23, 24] and H_2O_2 formation was quantified at 571 nm by recording the spectrum of resorufin after 1 minute of incubation for each time point. In the absence of benzydamine all the steps were identical, but the reactions were not subjected to HPLC. In order to assess if benzydamine can be oxidized non-enzymatically by H_2O_2 a reaction control was performed by incubating 20 µM of with benzydamine at 37°C for 1 hour. The concentration of was chosen to reproduce the highest amount of present in the reaction mixture produced by the enzyme.

For superoxide radical detection, in order to exclude that the signal of cytochrome c reduction is not due to superoxide, 2 control reactions were performed. In the first control, the cytochrome c reduction experiment was performed in the presence of SOD using 10 μM of cytochrome c. Figure S4, clearly shows that at this cytochrome c concentration there is no direct cytochrome c reduction by the enzyme. In the second control, cytochrome c reduction was performed in the absence/presence of SOD using 50 μM of cytochrome c. The data presented in Figure S5, demonstrate that at this higher cytochrome c concentration there is a contribution of hFMO3 to direct cytochrome c reduction. Therefore, only the SOD inhibited part of the signal can be used to measure superoxide. The amount of superoxide matches what was previously found using 10 μM cytochrome c that is the optimal concentration to test cytochrome c reduction without the interference of direct reduction from hFMO3 by cytochrome c.

To calculate the amount of superoxide produced by hFMO3 an extinction coefficient of 2.1x10^4 $M^{-1}cm^{-1}$ was used which is the difference in the extinction coefficients between the reduced and oxidized forms and it was used because it takes into account only the amount of superoxide that is actually formed during the reaction. All analyses were carried out using 10 μM horse heart cytochrome c (Sigma).

2.3 HPLC analysis

N-oxygenation of benzydamine by the wild type and N61S variant of hFMO3 were carried out as previously described [24, 25] and the amount of product determined by HPLC (Agilent-1200, Agilent Technologies, U.S.A.). Each sample was analyzed by HPLC equipped with 4.6×150 mm 5 μm Eclipse XDB-C18 column at room temperature with the UV–visible detector set at 308 nm for benzydamine N-oxide as described previously [25].

151 2.4 Calculation of the percentage of uncoupling

152

153 Uncoupling percentages were calculated by dividing the absolute rates of the rates of
154 benzydamine oxidation by the NADPH consumption which yields the coupled reaction. The
155 uncoupled reaction is given by the subtraction of the coupled reaction from the total reaction
156 (including both coupled and uncoupled reactions).

157

158 2.5 Differential scanning calorimetry

159 In order to provide direct effects of hydrogen peroxide exposure differential scanning
160 calorimetry experiments were carried out for hFMO3 following incubation of the enzyme with
161 hydrogen peroxide. Differential scanning calorimetry was carried out as previously illustrated
162 [13]

163

164 2.6 Statistical analyses

165 Statistical analyses were performed using Sigmaplot 11.0 software. Data calculations were
166 carried out by repeated-measures of two-way ANOVA followed by Student-Newman-Keuls post
167 hoc test. All experiments were executed in triplicates. Data are shown as mean ± standard
168 deviation. Differences among data points were considered significant when $p < 0.05$.

169

170 **3. Results**

171 In order to measure the uncoupling reactions of hFMO3, the NADPH oxidation activity of the
172 purified WT enzyme was investigated by monitoring the kinetics of the decrease in absorbance
173 of the reduced cofactor at 340 nm in time. NADPH by itself shows minimal oxidation in the
174 absence of the enzyme, so the reaction can actually start only when both NADPH and hFMO3

are present (data not shown). The amount of H_2O_2 produced was measured by mixing aliquots of each reaction, at different times after the start, with the AMPLEX red kit components [23]. We compared the H_2O_2 produced by WT hFMO3 and its polymorphic variant, N61S. The latter, an active site mutant associated with trimethylaminuria is known to have impaired $NADP^+$ binding and lower activity [13]. The data obtained demonstrate how in the absence of the substrate benzydamine (BZD), N61S produces higher amounts of H_2O_2 compared to WT (Fig 1). Interestingly WT showed steadily increased leakage while N61S had high leakage at the beginning of the incubation that decreased slowly after the first 15 minutes.

A) B)

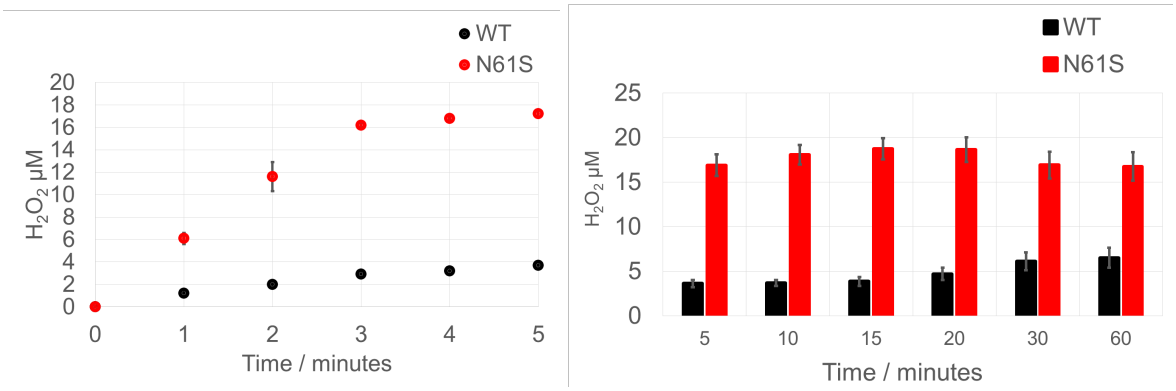

Fig. 1. H_2O_2 generation for WT and N61S hFMO3. The amount of hydrogen peroxide was measured for WT (black) and N61S mutant (red) hFMO3 as a function of time after the reaction is started. A) Generation of hydrogen peroxide in the first 5 minutes. B) Generation of hydrogen peroxide for 60 minutes. Reaction conditions for the production of hydrogen peroxide: 1.6 µM hFMO3 with 160 µM NADPH at 37°C in the dark in 50 mM KPi at pH 7.4. For detection of hydrogen peroxide refer to Materials and Methods.

If we look at the overall rate of H_2O_2 production by hFMO3 (Fig 2) the data are in agreement with recently published data [16] for this enzyme (0.5–2.5 nmol/min/nmol FMO at pH 7.4).

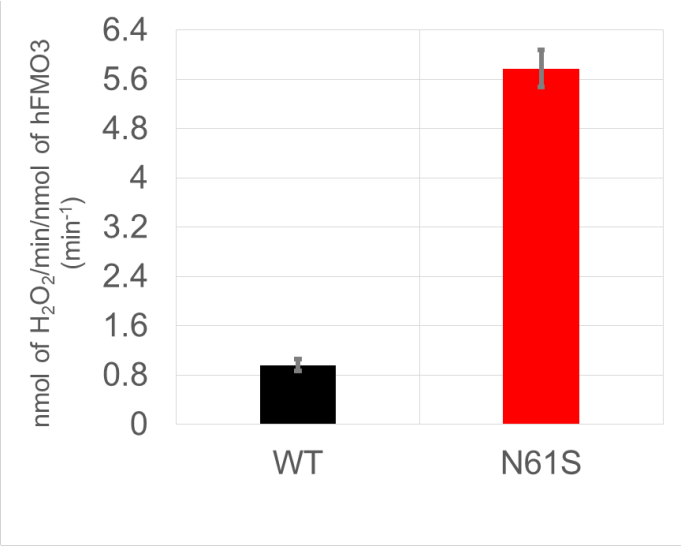

Fig. 2. Rate of H_2O_2 formation. Calculation of the rate is performed using the linear range of the kinetics curve between 60 and 180 seconds. Reaction conditions for the production of hydrogen peroxide: 1.6 μM hFMO3 and 160 μM NADPH at 37°C in the dark in 50 mM KPi, pH 7.4.

Moreover, in order to better understand what is the real level of uncoupling in hFMO3, we also measured the amount of product (benzydamine N-oxide) formed as a function of NADPH consumed. As expected the WT enzyme shows overall lower uncoupling (50-70%) when compared to N61S (90-95%), as shown in Figure 3.

A) B) C)

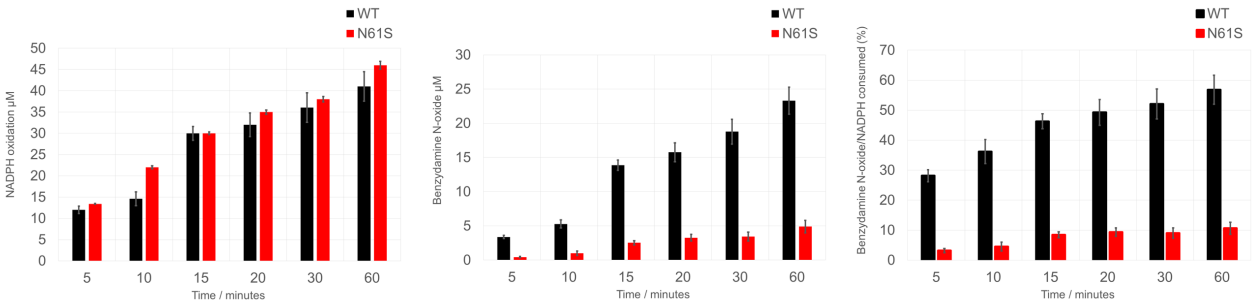

Fig. 3. Enzyme coupling efficiency. A) Oxidation of NADPH B) Product formation measured as benzydamine N-oxide C) Ratio between the amount of benzydamine N-oxide formed and the amount of NADPH consumed for WT (black) and N61S mutant (red) hFMO3. Reaction conditions for the production of hydrogen peroxide: 1.6 μM hFMO3, 160 μM NADPH with 300 μM benzydamine at 37°C in the dark in 50 mM KPi at pH 7.4.

Further characterization of the uncoupling process was carried out by measuring H_2O_2 production under different conditions to assess the specific contribution of the substrate benzydamine (BZD), in the presence of catalase (CAT) and superoxide dismutase (SOD). For both WT and N61S enzymes the presence of substrate significantly lowers the formation of H_2O_2 (Figure 4A, B, Figure S6). As expected, catalase totally removed the H_2O_2 from the reaction mixtures, so no H_2O_2 was detected (data not shown). On the other hand, superoxide dismutase in the absence of substrate, increased the amount of H_2O_2 detected after 15 and 30 minutes suggesting the possible formation of superoxide radical (i.e. since superoxide dismutase catalyzes the disproportionation of superoxide into O_2 and H_2O_2, an increase in H_2O_2 is indicative of the presence of the superoxide radical) (Figure 4A).

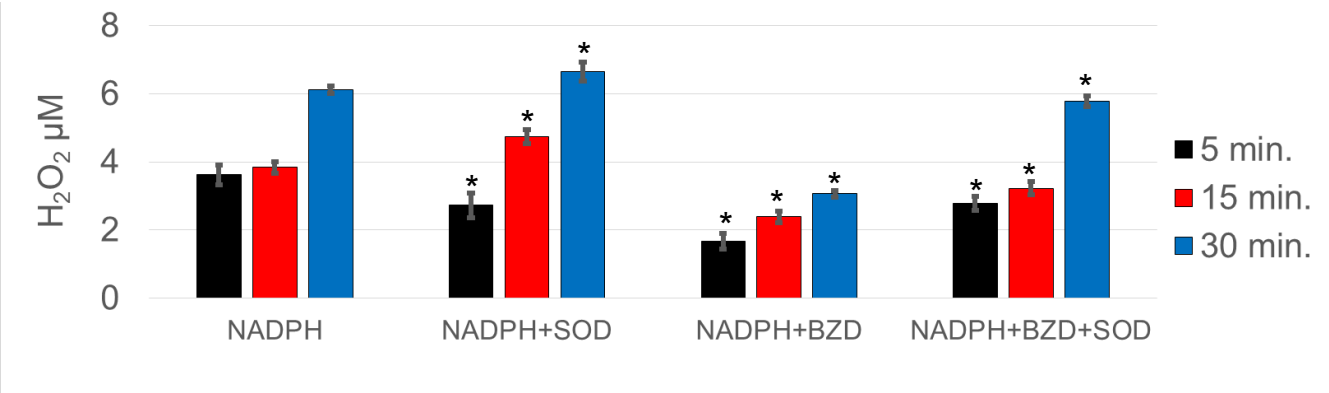

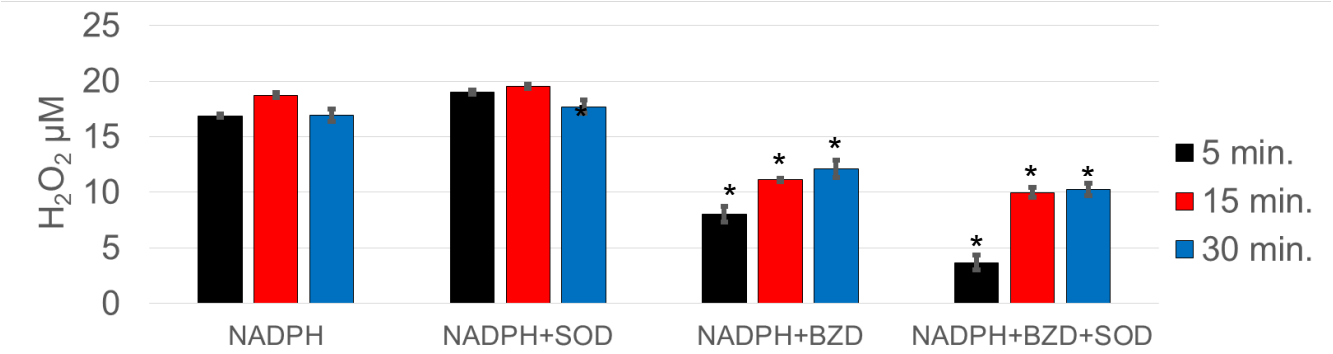

Fig. 4. Effect of substrate, catalase (CAT) and superoxide dismutase (SOD) on H_2O_2 generation. Data obtained WT (top) and N61S (bottom) hFMO3 after 5 (black), 15 (red) or 30 (blue) minutes. Bars represent the mean ± standard deviation. Statistically different (*) from same time of different group, $p < 0.05$. Reaction conditions: 1.6 µM hFMO3, 160 µM NADPH, 2 µM SOD with 2 µM catalase at 37°C in the dark in 50 mM KPi at pH 7.4.

Subsequently, the amount of benzydamine N-oxide product formed in the absence or presence of catalase/superoxide dismutase was also calculated. For WT both catalase and superoxide dismutase have a slightly negative impact after 15 minutes on the amount of product formed (Figure 5A). In the case of N61S variant, catalase has a positive impact on catalysis after 15 minutes whereas superoxide dismutase does not seem to affect product formation.

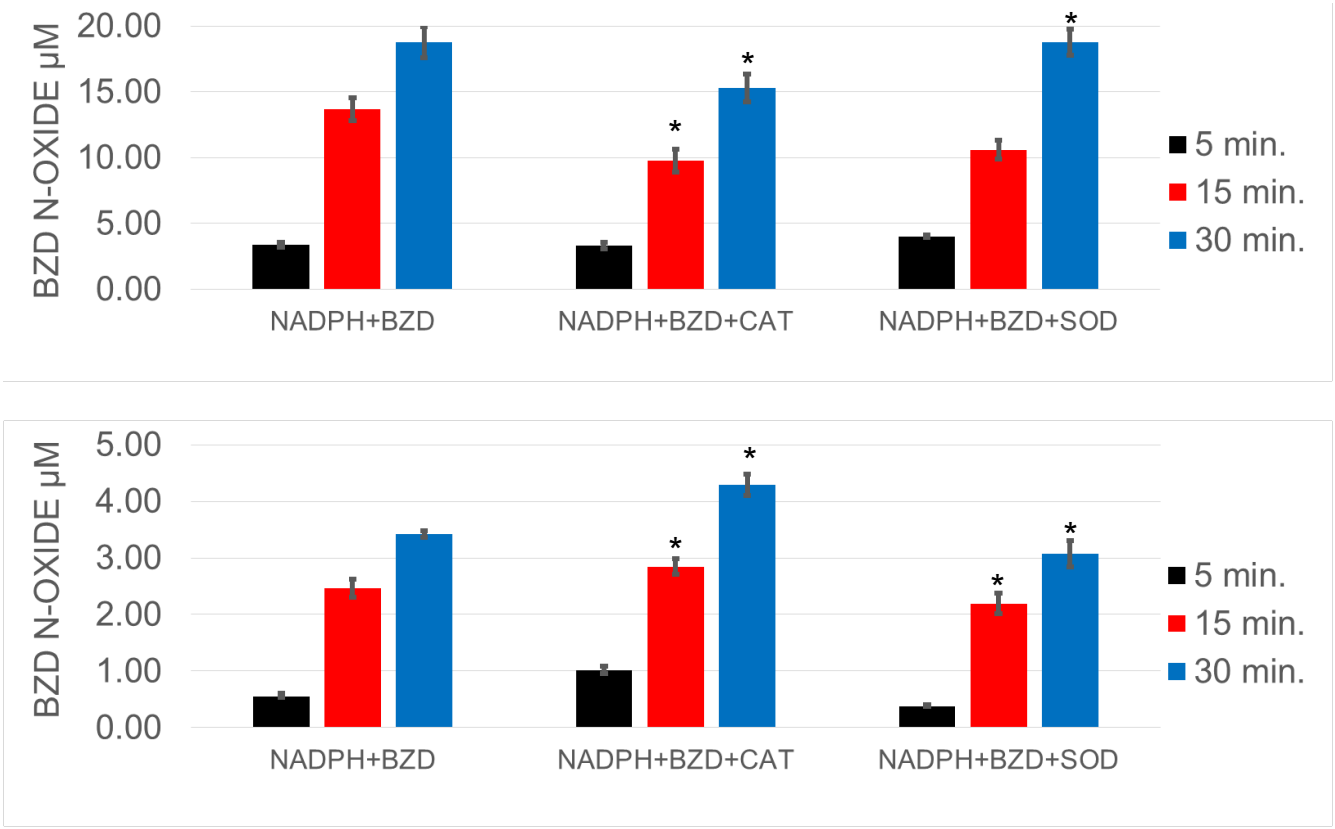

Fig. 5. Effect of substrate, catalase (CAT) and superoxide dismutase (SOD) on benzydamine N-oxide product formation. Data obtained WT (top) and N61S (bottom) hFMO3 after 5 (black), 15 (red) or 30 (blue) minutes. Bars represent the mean ± standard deviation. Statistically different (*) from same time of different groups, $p < 0.05$. Reaction conditions: 1.6 µM hFMO3, 160 µM NADPH, 300 µM benzydamine, 2 µM SOD and 2 µM catalase at 37°C in the dark in 50 mM KPi at pH 7.4.

Given the above measured contribution of superoxide dismutase to H_2O_2 production and to clarify whether hFMO3 can actually form the superoxide radical, a cytochrome c reduction assay was carried out [17]. The control reaction was performed using superoxide dismutase to

eliminate any source of superoxide (data not shown). As shown in Figure 6, cytochrome c reduction clearly shows how both WT and N61S hFMO3 are able to form the superoxide radical and that N61S forms twice as much superoxide reaching 4 μM after 5 minutes.

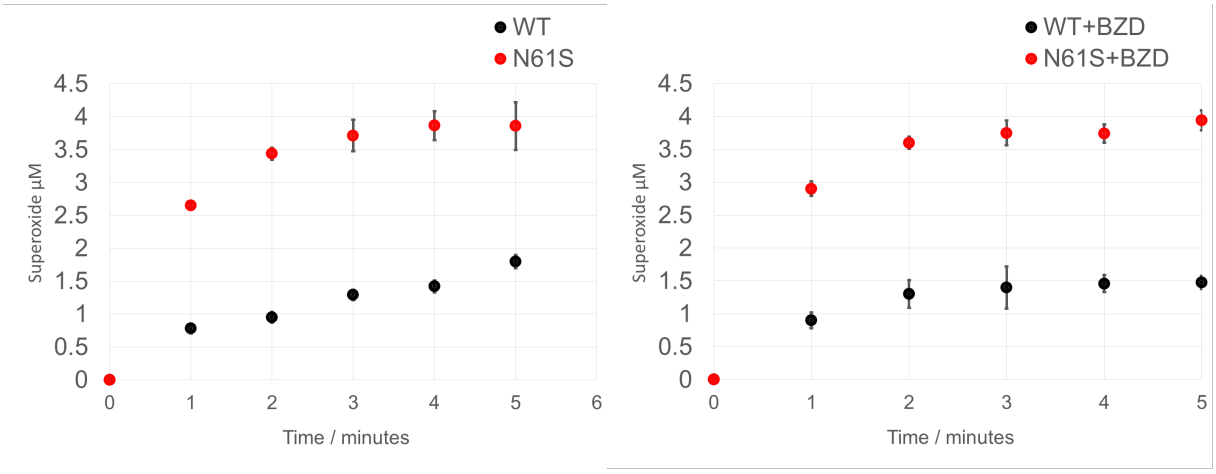

Fig. 6. Generation of superoxide. WT (black) and N61S mutant (red) hFMO3. A) Cytochrome c reduction in the absence of benzydamine. B) Cytochrome c reduction in the presence of benzydamine. Reaction conditions: 1.6 μM hFMO3, 160 μM NADPH, 300 μM benzydamine, 10 μM cytochrome c with 2 μM SOD at 37°C in the dark in 50 mM KPi at pH 7.4.

Finally, taken all the data together the total amount of uncoupling measured for both hFMO3 and its N61S polymorphic variant was converted into percentages (see Materials and methods section). In the case of the WT enzyme, after 10 min of incubation with the substrate, ~62% uncoupling was calculated of which 48% is due to hydrogen peroxide with remaining 14% due to superoxide radical formation. On the other hand, under the same experimental conditions, the N61S polymorphic variant is ~98% uncoupled with 80% from hydrogen peroxide and 18% from superoxide formation.

4. Discussion

Mechanistic studies carried out on pig liver FMO during the 1980's pointed unequivocally towards a precise scheme: mammalian FMO is reduced by NADPH and upon binding of oxygen can form a stable C4a-hydroperoxide intermediate [11,12]. It has been postulated that FMO is present in the cell in this highly reactive form ready to exert catalysis on its substrates [27, 28]. Such mechanism was also investigated against a large number of substrates and even though the enzyme shows differential affinity for N- or S- soft nucleophiles, it is thought to lack a proper binding step during catalysis. According to this scheme, any suitable molecule can be monooxygenated by FMO, provided that charge and size characteristics are respected [27].

In this context, the uncoupling reactions of FMO and its ability to generate reactive oxygen species has been considered negligible for a long time. Nevertheless, more recent studies have highlighted the fact that hFMO3 does not form a highly stable C4a-hydroperoxy intermediate [13]. UV-vis stopped-flow experiments demonstrated that WT hFMO3 forms an intermediate that can last for minutes and not for hours [13, 14]. Further characterization of the enzyme led to the confirmation that $NADP^+$ binding is crucial for the intermediate stability and that an active site mutant, N61S, dramatically decreases the affinity of the enzyme for the cofactor preventing the formation of the reaction intermediate [13, 14]. Measured K_d values for NADPH are 0.3 and 51.8 μM for WT and N61S hFMO3, respectively [13]. In the case of NADP+ the binding affinity for WT is 3.7 μM, whereas for N61S no appreciable binding could be detected [13].

Other published studies on hFMO5 have also pointed towards the absence of a stable intermediate in the reaction mechanism of the enzyme and suggested the unproductive leakage of the peroxyflavin [15]. In a recent published work by Williams and colleagues [16] the uncoupling process of human FMO isoforms 1, 2 and 3 was studied. The latter authors

300 demonstrated how all studied isoforms generate H_2O_2 upon reduction by NADPH, both in the
301 presence or absence of substrate and, unexpectedly that the presence of substrate even
302 increased the amount of H_2O_2 generated by FMO [16]. The same group did not observe any
303 effect with the addition of catalase or superoxide dismutase to the reaction [16].
304 In this work, we undertook an extensive characterization of hFMO3 on the basis of the above-
305 mentioned recent findings. For this reason, two purified enzymes were used: wild type hFMO3
306 and N61S [13]. It was found that both WT and N61S produce H_2O_2 (Figure 1) with higher
307 amounts observed with the mutant due to the its inability to bind $NADP^+$ and form a stable C4a-
308 hydroperoxy intermediate. The latter finding suggests that this mutation leads to an overall
309 faster catalytic cycle that is detrimental for catalysis [13]. This is fully in line with previous
310 characterization of the rates of formation and decay of the flavin intermediates reported for WT
311 and N61S hFMO3 [13].
312 Subsequently, we focused our attention to the actual meaning of coupling i.e. the use of
313 electrons donated by NADPH to yield a product molecule. To this end, benzydamine a hFMO3
314 marker substrate was used and the amount of product was measured as a percentage of the
315 NADPH consumed. The data confirmed a high degree of uncoupling for hFMO3 and an even
316 higher increased propensity to the unproductive leakage of electrons for the N61S variant
317 (Figure 3). More importantly, if the amount of H_2O_2 produced in the absence/presence of the
318 substrate is compared, it becomes evident that the presence of the substrate results in a strong
319 decrease in the amount of H_2O_2 (Figure 4A, B). The latter observation is actually in line with the
320 current representation of the catalytic cycle [16].
321 All these findings indicate that there are competing paths that ultimately lead to the regeneration
322 of the FAD cofactor: the productive path leads to product oxidation with the unproductive path
323 leading to the formation of reactive oxygen species. Further analysis shows that both catalase

and superoxide dismutase slightly decrease the amount of benzydamine N-oxide formed in the enzymatic reaction for WT and have contrasting effects for N61S (Figure 5A, B). A possible explanation for the increase in product formation for WT is that N-oxidation can be achieved - at least to a much lower extent - in the absence of enzyme and only by H_2O_2, as most N-oxides are actually synthetized [29]. Nevertheless, our experiments show that incubation of H_2O_2 with benzydamine does not lead to non-enzymatic product formation (Figure S7). In the case of N61S, a significant increase in the amount of product is detected after 30 minutes in presence of catalase. This could be due to the decreased protein structural damage caused by large amounts of H_2O_2 in the absence of catalase after several minutes/catalytic cycles. Our data indicate that incubation of H_2O_2 with hFMO3 does not lead to structural damage (Figure S8). Therefore the increased amount of product formed for N61S can only be compatible with a higher coupling efficiency in the presence of catalase.

In general, looking at the catalytic cycle of hFMO3 (Fig. 7) a productive oxidative half-cycle leading to N-oxidation of the substrate and an unproductive oxidative half-cycle leading to H_2O_2 can clearly be identified. As expected in the presence of the substrate the enzyme uses the productive path more often as confirmed by data obtained in presence of benzydamine showing that the presence of this substrate favors the coupled reaction and decreases the amount of H_2O_2 formed. Moreover, since a higher amount of H_2O_2 was observed in the presence of superoxide dismutase, the possibility of hFMO3 producing the superoxide radical was also investigated. Cytochrome c reduction experiments confirmed hFMO3 as the source of superoxide radical. As mentioned earlier, superoxide radical formation had already been reported for pig FMO but it had been studied in close association to the possible exploitation of this reactive oxygen species for the hydroxylation of amines [17] and not in the context of the uncoupling reactions.

In light of the observed superoxide radical, we propose a second shunt in the catalytic cycle of hFMO3 consisting of an earlier exit from the productive path (fig. 7, steps a, b). The latter is in addition to the already reported shunt leading to H_2O_2 (fig. 7, step c) as mentioned above [16]. It is known that for the reduced flavin to react with oxygen a “radical pair” between the superoxide and the flavin semiquinone is formed (fig. 7 step 2) [30]. This species is highly unstable and it has never been captured [31], but it is chemically required to bypass the spin inversion barrier [30, 31]. At this point of the cycle the radical pair can either yield the hydroperoxyflavin (fig. 7 step 3-4) or take an unproductive path and generate a semiquinone radical with the loss of the superoxide (fig. 7 step a). This semiquinone intermediate can decay resulting in the re-oxidized flavin with the concomitant production of another superoxide (fig. 7 step b). This new path can explain why after the formation of the caged radical pair, superoxide can detach from the flavin together with $NADP^+$, short circuiting the catalytic cycle.

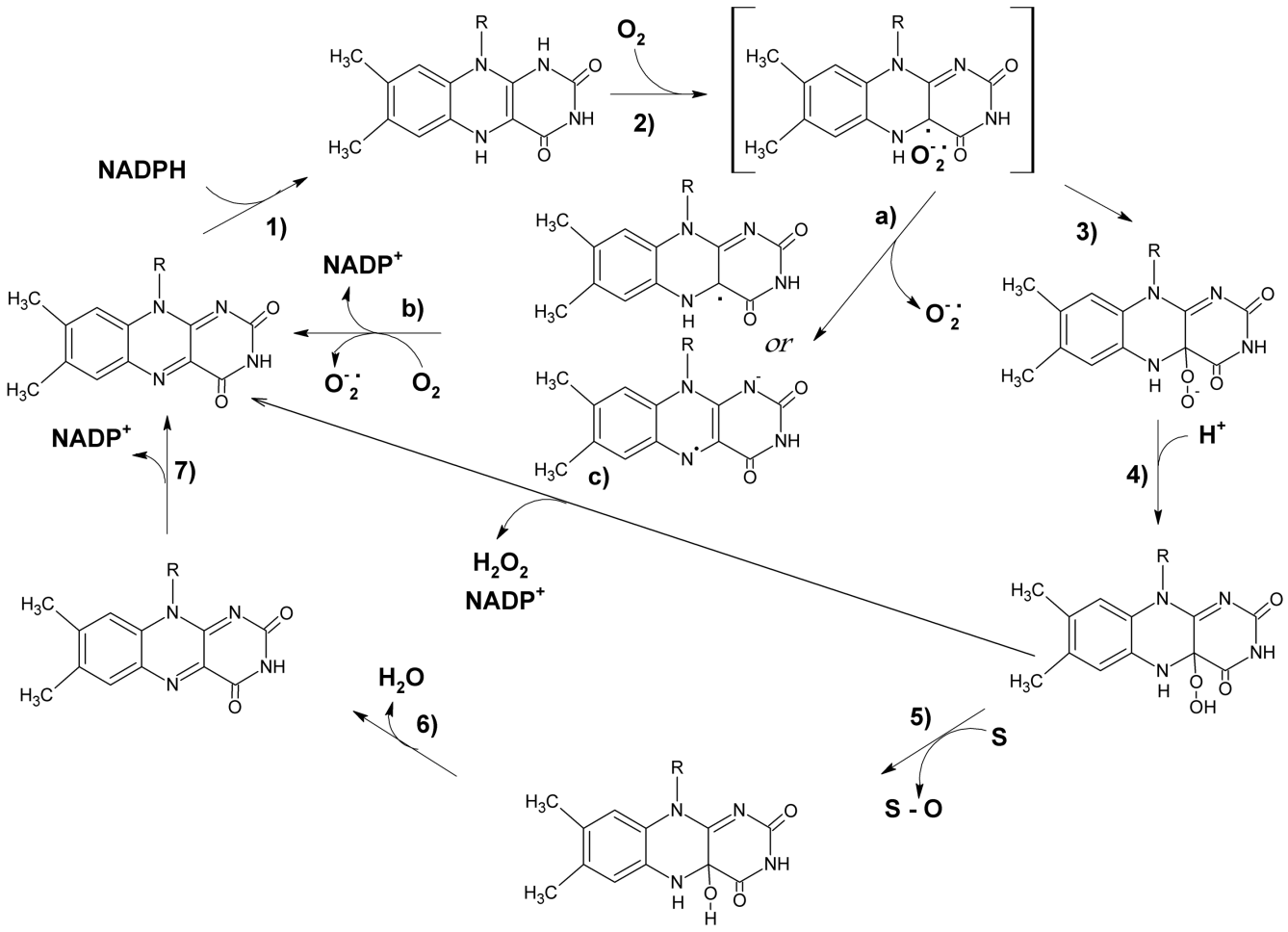

Fig. 7. Chemical structures of FAD reaction intermediates during the catalytic cycle of flavin-containing monooxygenases. NADPH reduction (step 1) is rapidly followed by activation of molecular oxygen (step 2), binding on the C4a and protonation to yield the C4a-hydroperoxide (step 3-4). This intermediate can react with the substrate (S) and yield the oxygenated product (S-O, step 5). The second atom of oxygen is released as H_2O (step 6) and $NADP^+$ can leave the active site (step 7). Two side reactions can occur that produce reactive oxygen species: steps a) and b) before formation of the hydroperoxyflavin after spin inversion of the radical pair which can result in the loss of superoxide or step c) the direct loss of H_2O_2 from the C4a-hydroperoxy intermediate.

The physiological role of the uncoupled reaction products of hFMO3 is still unknown. It has been suggested that the generation of hydrogen peroxide by FMO could play a role in control of the overall redox state of the cell [27] or in the synthesis of protein disulfide bonds through cysteamine oxidation [32, 33]. On the other hand, toxicological effects such as hepatic injury through radical production and lipid peroxidation have also been reported in rat FMO catalyzing the oxidation of thioacetamide [34]. Initially it was thought that the products of thioacetamide, being radicals themselves, were initiating the inflammation and the resulting hepatic injury, but further investigation suggested the FMO enzyme itself might be involved [35]. Nevertheless, since this current work and others [16-18] have shown FMO enzymes to be highly uncoupled, further studies are required to confirm whatever the role of these reactive oxygen species maybe, physiological or toxicological.

Conflict of interest

The authors declare no conflict of interest

Acknowledgement

Chongliang Gao is the recipient of a PhD scholarship from University of Torino for international students. This research did not receive any specific grant from funding agencies in the public, commercial, or not-for-profit sectors.

References

[1] J.R. Cashman and J. Zhang, Human Flavin-Containing Monooxygenases. Ann. Rev. Pharmacol. Toxicol. 46 (2006) 65–100.

[2] I.R. Philips and E.A. Shephard, Drug metabolism by flavin-containing monooxygenases of human and mouse. Exp. Opin. Drug Metab. Toxicol. 13 (2017) 167–181.

[3] L. L. Poulsen and D. M. Ziegler, The liver Microsomal FAD-containing Monooxygenase J. Biol. Chem. 254, (1979) 6449-6455.

[4] D.H. Lang, C.K. Yeung, R.M. Peter, C. Ibarra, R. Gasser, K. Itagaki, R.M. Philpot, A.E. Rettie, Isoform specificity of trimethylamine N-oxygenation by human flavin-containing monooxygenase (FMO) and P450 enzymes - Selective catalysis by FMO3, Biochemical Pharmacology 56(8) (1998) 1005-1012.

[5] J.R. Cashman, Y.A. Bi, J. Lin, R. Youil, M. Knight, S. Forrest, E. Treacy, Human flavin-containing monooxygenase form 3: cDNA expression of the enzymes containing amino acid substitutions observed in individuals with trimethylaminuria, Chemical Research in Toxicology 10(8) (1997) 837-841.

[6] C.T. Dolphin, A. Janmohamed, R.L. Smith, E.A. Shephard, I.R. Phillips, Missense mutation in flavin-containing mono-oxygenase 3 gene, FMO3, underlies fish-odour syndrome, Nature Genetics 17(4) (1997) 491-494.

[7] C.T. Dolphin, A. Janmohamed, R.L. Smith, E.A. Shephard and I. R. Phillips, Compound heterozygosity for missense mutations in the flavin-containing monooxygenase 3 (FMO3) gene in patients with fish-odour syndrome. Pharmacogen. 10 (2000) 799–807.

[8] Z. Wang, E. Klipfell, B.J. Bennett, R. Koeth, B.S. Levison, B. Dugar, A.E. Feldstein, E.B. Britt, X. Fu, Y.-M. Chung, Y. Wu, P. Schauer, J.D. Smith, H. Allayee, W.H.W. Tang, J.A. Di Donato, A.J. Lusis, S.L. Hazen, Gut flora metabolism of phosphatidylcholine promotes

418 cardiovascular disease, Nature 472 (2011) 57-82.
419 [9] C. Johnson, A.J. Prokopienko, R.E. West, T.D. Nolin, J.R. Stubbs, Decreased Kidney
420 Function Is Associated with Enhanced Hepatic Flavin Monooxygenase Activity and
421 Increased Circulating Trimethylamine N-Oxide Concentrations in Mice, Drug Metabolism
422 Disposition 46(9) (2018) 1304-1309.
423 [10] J.A.P. Tomlinson, D.C. Wheeler, The role of trimethylamine N-oxide as a mediator of
424 cardiovascular complications in chronic kidney disease, Kidney International 92(4) (2017)
425 809-815.
426 [11] N.B. Beaty and D.P. Ballou, The Reductive Half-reaction of Liver Microsomal FAD-
427 containing Monooxygenase, Journal of Biological Chemistry, 256(9) (1981) 4611-4618.
428 [12] N.B. Beaty and D.P. Ballou, The Oxidative Half-reaction of Liver Microsomal FAD-
429 containing Monooxygenase, 256(9) (1981) 4619-4625.
430 [13] C.L. Gao, G. Catucci, S. Castrignano, G. Gilardi, S.J. Sadeghi, Inactivation mechanism of
431 N61S mutant of human FMO3 towards trimethylamine, Scientific Reports 7 (2017).
432 [14] C. Gao, G. Catucci, G. Gilardi, S.J. Sadeghi, Binding of methimazole and NADP(H) to
433 human FMO3: In vitro and in silico studies, Int. J. Biol. Marcromol. 118 (Part A) (2018) 460-
434 468.
435 [15] F. Fiorentini, M. Geier, C. Binda, M. Winkler, K. Faber, M. Hall, A. Mattevi, Biocatalytic
436 Characterization of Human FMO5: Unearthing Baeyer-Villiger Reactions in Humans, ACS
437 Chemical Biology 11(4) (2016) 1039-1048.
438 [16] L.K. Siddens, S.K. Krueger, M.C. Henderson, D.E. Williams, Mammalian flavin-containing
439 monooxygenase (FMO) as a source of hydrogen peroxide, Biochemical Pharmacology
440 89(1) (2014) 141-147.
441 [17] E.J. Rauckman, G.M. Rosen, B.B. Kitchell, Superoxide Radical as an Intermediate in the

442 Oxidation of Hydroxylamines by Mixed Function Amine Oxidase, Molecular Pharmacology
443 15(1) (1979) 131-137.
444 [18] R.E. Tynes, P.J. Sabourin, E. Hodgson, R.M. Philpot, Formation of hydrogen peroxide and
445 N-hydroxylated amines catalyzed by pulmonary flavin-containing monooxygenases in the
446 presence of primary alkylamines, Archives of Biochemistry and Biophysics 251(2) (1986)
447 654-664.
448 [19] G. Catucci, G. Gilardi, L. Jeuken, S.J. Sadeghi, In vitro drug metabolism by C-terminally
449 truncated human flavin-containing monooxygenase 3, Biochemical pharmacology 83(4)
450 (2012) 551-8.
451 [20] S.J. Sadeghi, R. Meirinhos, G. Catucci, V.R. Dodhia, G. Di Nardo, G. Gilardi, Direct
452 Electrochemistry of Drug Metabolizing Human Flavin-Containing Monooxygenase:
453 Electrochemical Turnover of Benzydamine and Tamoxifen. J. Am. Chem. Soc. 132 (2010)
454 458-59.
455 [21] G. Catucci, S.J. Sadeghi, G. Gilardi, A direct time-based ITC approach for substrate
456 turnover measurements demonstrated on human FMO3,
457 Chemical Communications, 55 (2019) 6217-6220.
458 [22] G. Catucci, I. Polignano, D. Cusumano, C. Medana, G. Gilardi, S.J. Sadeghi, Identification
459 of human flavin-containing monooxygenase 3 substrates by a colorimetric screening assay,
460 Analytical Biochemistry 522 (2017) 46-52.
461 [23] V. Mishin, J.P. Gray, D.E. Heck, D.L. Laskin, J.D. Laskin, Application of the Amplex
462 red/horseradish peroxidase assay to measure hydrogen peroxide generation by
463 recombinant microsomal enzymes, Free Radical Biology and Medicine 48(11) (2010) 1485-
464 1491.
465 [24] G. Catucci, I. Zgrablic, F. Lanciani, F. Valetti, D. Minerdi, D.P. Ballou, G. Gilardi, S.J.

Sadeghi, Characterization of a new Baeyer-Villiger monooxygenase and conversion to a solely N-or S-oxidizing enzyme by a single R292 mutation, Biochimica Biophysica Acta-Proteins and Proteomics 1864(9) (2016) 1177-1187.

[25] G. Catucci, S. Bortolussi, G. Rampolla, D. Cusumano, G. Gilardi, SJ Sadeghi Flavin-Containing Monooxygenase 3 Polymorphic Variants Significantly Affect Clearance of Tamoxifen and Clomiphene, Basic and clinical pharmacology and toxicology, 123 (2018) 687-691.

[26] S. Castrignano, S. Bortolussi, G. Catucci, O. Gholami, F. Valetti, G. Gilardi, S.J. Sadeghi, Bioelectrochemical profiling of two common polymorphic variants of human FMO3 in presence of graphene oxide, Electrochimica Acta 228 (2017) 611-618.

[27] S.K. Krueger, D.E. Williams, Mammalian flavin-containing monooxygenases: structure/function, genetic polymorphisms and role in drug metabolism, Pharmacology & Therapeutics 106(3) (2005) 357-387.

[28] G. Catucci, C.L. Gao, S.J. Sadeghi, G. Gilardi, Chemical applications of Class B flavoprotein monooxygenases, Rendiconti Lincei-Scienze Fisiche E Naturali 28 (2017) 195-206.

[29] K. Bergstad, J.E. Backvall, Mild and efficient flavin-catalyzed H2O2 oxidation of tertiary amines to amine N-oxides, Journal of Organic Chemistry 63(19) (1998) 6650-6655.

[30] V. Massey, Activation of molecular-oxygen by flavins and flavoproteins, Journal of Biological Chemistry 269(36) (1994) 22459-22462.

[31] P. Chaiyen, M.W. Fraaije, A. Mattevi, The enigmatic reaction of flavins with oxygen, Trends in Biochemical Sciences 37(9) (2012) 373-380.

[32] L.L. Poulsen, D.M. Ziegler, Microsomal mixed-function oxidase-dependent renaturation of reduced ribonuclease. Arch Biochem Biophys 183 (1977) 565–570.

[33] D. M. Ziegler, M. W. Duffel, L. L. Poulsen, Studies on the nature and regulation of the cellular thio:disulphide potential. Ciba Found Symp 72 (1979), 191– 204.

[34] P.V. Reddy, Ch.R. Murthy, P. Reddanna, Fulminant hepatic failure induced oxidative stress in nonsynaptic mitochondria of cerebral cortex in rats. Neurosci. Lett. 368, (2004) 15–20.

[35] D.Z. Hsu, P.Y Chu., Y.H. Li, V.R. Chandrasekaran., M.Y. Liu, Role of flavin-containing-monooxygenase-dependent neutrophil activation in thioacetamide-induced hepatic inflammation in rats. Toxicology 298, (2012) 52-58.